

# Chapter 3

## Resist Leaching and Water Uptake

One unique aspect of 193i lithography is the use of water situated between the final lens element and the resist. The resist stack (with or without topcoat) on the wafer is dynamically exposed through this water with the step-and-scan process. The photoacid generator (PAG), quencher, and other small molecular components of the resist may leach into this water. These leached components contaminate the water and may degrade resist performance. This contaminated water can additionally contaminate the lens and wafer stage of the scanner. To master these leaching problems, we must understand the dynamics of resist leaching, transportation of leached contaminants in the immersion water, and the impact of these contaminants on the lens during exposure.

Additionally, water can penetrate the topcoat and diffuse into the resist film. This penetration and diffusion of water can cause the topcoat or the resist to swell, which will affect their lithographic performance. This chapter specifically addresses the following issues: (1) leaching test methods, (2) leaching dynamics, (3) leaching with 193-nm exposure, (4) pre-rinse to partially remove leached contaminants, (5) lens contamination caused by resist leaching, and (6) water uptake in resist film.

### 3.1 Leaching Test Methods

A general approach to evaluating the leaching characteristics of a resist involves several steps. First, a puddle of DI water is formed on the surface of the resist stack. After a specific period of time, the water in the puddle is sent for analysis. This leaching test measures the amount of resist components that are leached into the water over time. Various methods of immersing the resist film and extracting the water sample have been developed and reported,<sup>1</sup> however, the results have been inconsistent with variability as high as 2–3x. So far, no standard test method or specifications for leaching have been accepted by the entire 193i community. However, these are worthwhile goals and more reliable methods continue to be sought.<sup>2</sup>

### 3.1.1 Water extraction

Figure 3.1 shows a simple water extraction test method.<sup>3</sup> Although this method is not recommended, it gives a basic example of water extraction. A beaker with a wide opening (crystallizing dish) holds a specific volume of DI water (Fig. 3.1(a)). A silicon wafer coated with resist or resist stack is placed face down covering the beaker mouth (Fig. 3.1(b)). The beaker and the wafer are flipped over and the water covers the resist surface (Fig. 3.1(c)). The immersion area or resist leaching area is equal to the size of the beaker opening. After a specific amount of time, the beaker is flipped back to its normal position and the water is collected for analysis (Fig. 3.1(d)). To investigate the time dependence of leaching, a series of experiments can be conducted as a function of retention time.

Two recommended methods for this investigation are the Water EXtraction and Analysis (WEXA) technique described by IBM<sup>4</sup> and the Dynamic Leaching Procedure (DLP) developed at IMEC.<sup>5</sup> Figure 3.2(a) shows a diagram of the bottom view of a Teflon lid in the WEXA design. In the test, the lid covers the resist surface and the evacuation hole is connected to a vacuum pump. The gap between the wafer and the lid is filled with water. Water flows along the rectangular channel, reaching the outlet. The contact time with water can be varied by adjusting the flow rate and the size of the channel. The water flowing out of the outlet hole is collected for analysis.

Figure 3.2(b) is a diagram of how the DLP works. A resist-coated wafer is loaded onto the wafer stage. A showerhead dispenses a specific volume of water across the resist surface. Then, the water in the showerhead is collected for analysis. The retention time of water contact can be varied by adjusting the speed.

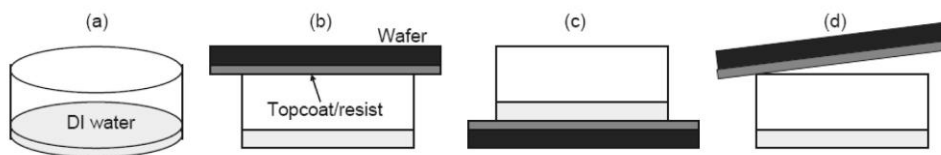


**Figure 3.1** Simple method of extracting a water sample from the resist surface using a crystallizing dish.

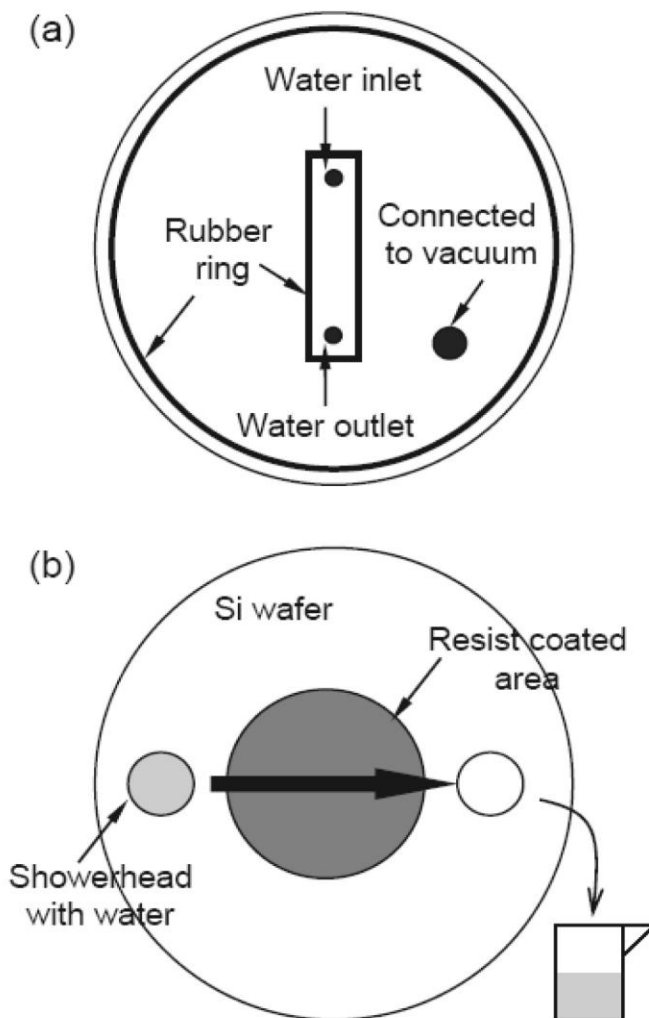


**Figure 3.2** Diagrams of (a) WEXA cover design (bottom view) and (b) how DPL works.

### 3.1.2 Water sample analysis

Water samples can be analyzed for resist components using various chemical analytical methods that have different sensitivities toward certain components. The best analytical method must be chosen for each compound. For example, sulfonates of PAG can be detected separately by liquid chromatography mass spectroscopy (LC-MS) with a detection limit of 0.2ng/mL or ppb. The dynamic leaching rate ( $\text{ng}/\text{cm}^2\text{s}$ ) can be determined from quantitative measurements, contact area, and immersion time. SEMATECH experiments suggest that the PAGs are most likely to leach from the film and also impose the greatest danger to the lens.<sup>6</sup> Experimental results from resist vendors also support this suggestion.

## 3.2 Leaching Dynamics

### 3.2.1 Leaching dynamics described by a single-exponential model

The rate of leaching has been shown to be nonlinear. The resist components (primarily PAGs) leach faster at the beginning of contact with water. Radioactive labeling studies and early kinetics studies with limited time resolution have shown that leaching reaches a limiting value within a few seconds after water contact.<sup>6</sup> The concentration  $C$  of PAG in water versus the water contact time  $t$  can be approximately described by an exponential relation:

$$C = C_{\infty} \cdot (1 - e^{-\beta t}), \quad (3.1)$$

where  $C_{\infty}$  is the saturated PAG concentration and  $\beta$  is the time constant.<sup>7</sup> The leaching rate  $dC/dt$  changes with time. At initial time  $t = 0$ , the leaching rate has the maximum value— $dC/dt|_{t=0} = C_{\infty} \cdot \beta$ , which is called the dynamic leaching rate. Both  $C_{\infty}$  and  $C_{\infty} \cdot \beta$  can be obtained from the  $C-t$  curve (Fig. 3.3).

### 3.2.2 Leaching dynamics described by double-exponential model

Detailed measurements and data analysis suggest that the best fit of the leaching-rate data is obtained using two exponential functions. This is known as the double-exponential model:<sup>5</sup>

$$C = C_{\infty 1} (1 - e^{-\beta_1 t}) + C_{\infty 2} (1 - e^{-\beta_2 t}) . \quad (3.2)$$

$C_{\infty 1} + C_{\infty 2}$  is the saturated concentration and  $\beta_1$  and  $\beta_2$  are the time constants. Figure 3.4 shows the leaching amount of anion from PAR-817 resist as a function of the water contact time. These results were measured via the DLP method at IMEC. Both the single-exponential model (Eq. (3.1)) and the double-exponential

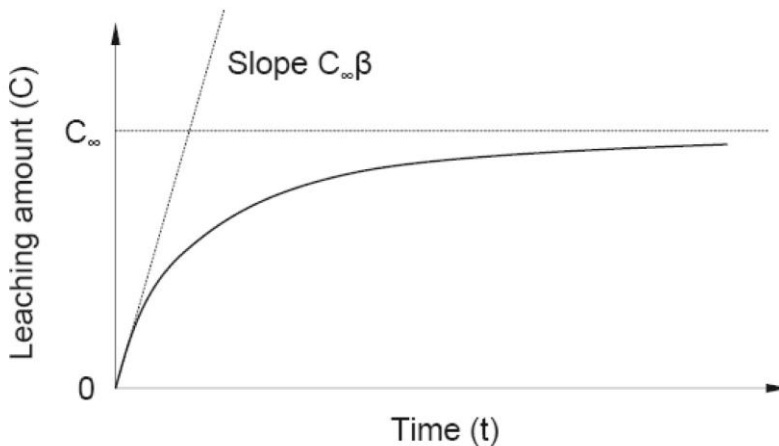
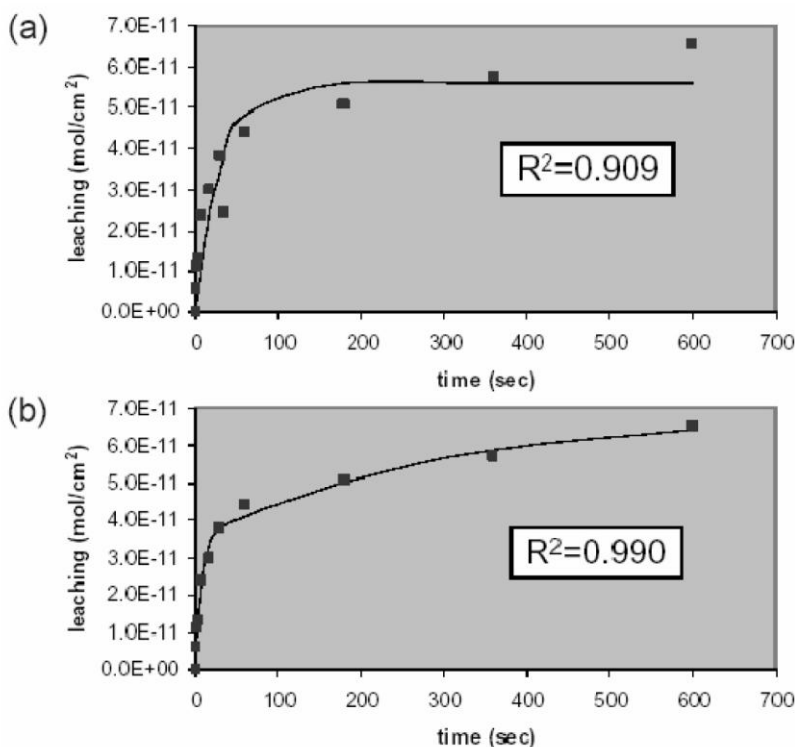


Figure 3.3 Dynamic model of PAG leaching.

model (Eq. (3.2)) were used to fit the measured data points shown in Figs. 3.4(a) and (b)). The correlation coefficients ( $R^2$ ) show that the double-exponential model fits the original data better than does the single-exponential model.

The double-exponential model suggests two processes, one fast and one slow, that could play a role in resist leaching. The fast leaching process occurs immediately after the water contacts the resist and reaches saturation within a few seconds, while the slow leaching process lasts much longer, up to 5–20 minutes. The fast process may be a result of PAG that has accumulated near the resist–air interface during spin-coating and baking. The slow process may be a result of PAG leaching from within the bulk of the resist.<sup>8</sup> This mechanism explains why some residual leaching can be observed even after long pre-soaks. Finite element modeling suggests that PAG initially located at the surface quickly diffuses into the water.<sup>9</sup> However, the diffusion coefficients of PAG in the bulk are much smaller than they are within the surface region. These results are consistent with the experimental observations that leaching is best described by two time constants (Eq. (3.2)). One corresponds to the leaching of PAGs from the surface, the other corresponds to the leaching of PAGs from the bulk.



**Figure 3.4** Leaching amount of anion from PAR-817 resist as a function of the water contact time (dots in the figures). The curve in (a) is the fitted results ( $C_{\infty} = 5.6 \times 10^{-11} \text{ mol/cm}^2$ ,  $\beta = 0.033 \text{ s}^{-1}$ ) using the single-exponential model. The curve in (b) is the fitted results ( $C_{\infty 1} = 3.5 \times 10^{-11} \text{ mol/cm}^2$ ,  $\beta_1 = 0.15 \text{ s}^{-1}$ ;  $C_{\infty 2} = 3.4 \times 10^{-11} \text{ mol/cm}^2$ ,  $\beta_2 = 0.0035 \text{ s}^{-1}$ ) using the double-exponential model. (Reprinted by permission from Ref. 5.)

In a full-field 193-nm immersion scanner, the exposure head stays in one field only for a few seconds. Therefore, the fast leaching process is a particularly important factor in understanding lens contamination. The single-exponential model and dynamic leaching rate proposed in Eq. (3.1) are sufficient for studying leaching kinetics relevant to lens contamination. The slow leaching occurs in the time scale of 1–20 minutes and may play a role in the formation of watermark defects.

### 3.2.3 Leaching specifications recommended by scanner suppliers

The dynamic leaching rate is a measure of how quickly a resist component leaches from the film at the instant it contacts water. This value is more important than the saturated leaching value in the manufacturing environment because the water, lens, and resist are in close proximity only for a short time before the water is flushed from the system. Immersion water flows continuously through the 193i scanners so that the leached components are flushed from the system. Therefore, the dynamic leaching rate is a better measure of the concentration of resist components in the water near the lens. Tolerances for dynamic leaching rate are a function of the exposure head design and water flow rate.

Table 3.1 shows dynamic leaching rate specifications published by Nikon and ASML. Nikon has designed an exposure head that allows the water to flow from the top (lens) to the bottom (resist surface).<sup>10</sup> Water is contaminated by the resist downstream from the lens, enabling Nikon to relax its early leaching specifications by a factor of 15. Hopefully, additional improvements in exposure head designs will enable additional relaxation of leaching specifications in the future.

### 3.2.4 Comparing saturation leaching results

Determining saturation leaching levels is much easier than determining dynamic leaching rates, since analytical measurements can be made offline to determine saturation values. Therefore, most 193-nm immersion researchers have in-house capabilities for measurement of saturation leaching levels of resist samples. However, the details of these techniques differ from site to site and the absolute values of saturated leaching generally differ. Nonetheless, correlations can be established. The leaching values of six resist samples were measured at two different locations. Figure 3.5 shows the results obtained at one location plotted

**Table 3.1** Leaching rates suggested by scanner suppliers.<sup>10,1</sup>

	ASML	Nikon
PAG leaching	$1.6 \times 10^{-12}$ mol/cm <sup>2</sup> /s	$5 \times 10^{-12}$ mol/cm <sup>2</sup> /s
Amine leaching	-	$2 \times 10^{-12}$ mol/cm <sup>2</sup> /s

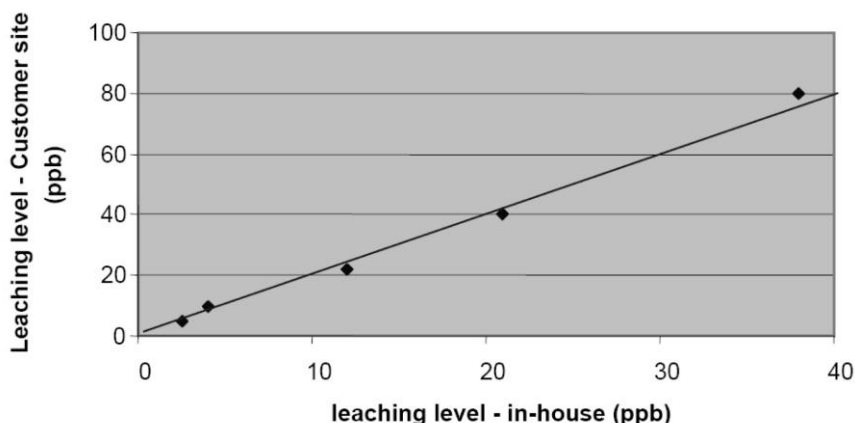


**Figure 3.5** Leaching test results comparison between different sites for same samples.

against results obtained at the other. The absolute values of the results tested in one location differ from those tested at the other location, but there is a linear correlation between the two sets of results. For the same resist sample, the PAG leaching level measured at one site is about 2x that of the other. These results show that it is possible to calibrate the leaching results between sites.

### 3.3 Leaching with 193-nm Exposure

The leaching tests discussed so far in this chapter were done without exposure. With exposure to 193-nm light, it is reasonable to expect that leaching levels increase. Unfortunately, to collect water samples directly after exposure is not easy and requires a special setup (Fig. 3.6). A small volume of DI water is dispensed and confined on the resist surface, forming a puddle. The apparatus controls the exposure area and exposes the resist through the water.

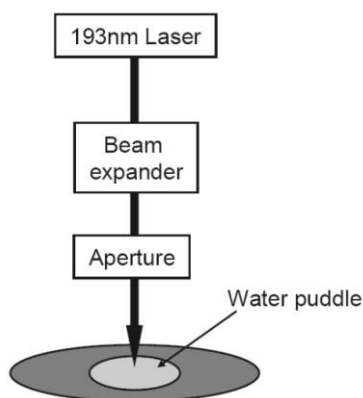


**Figure 3.6** Exposure system for leaching water collection.

In one study, a variety of resists or resist/topcoat stacks were exposed with different doses and evaluated for leaching. After exposure, water samples were collected and analyzed (Fig. 3.7). The PAG components of C1 and C4 were traced. Topcoat TC1 is such an effective leaching barrier that no leaching was detected, even at the exposure doses as high as  $3E_0$ . The leaching was higher without topcoat. With increased doses from 0 to  $3E_0$ , all data, except for resist1/TC1 stack, showed more C1 and C4 leached into water. However, the increased value is less than 15%.

The results in Fig. 3.7 suggest that leaching with exposure is about 15% higher than without exposure. Surprisingly, exposure to 193-nm light does not dramatically increase leaching. Similar results were reported for leaching levels of three resist stacks.<sup>12</sup> Exposure increased leaching levels by only 25–100% over unexposed samples. For this reason, scanner suppliers have agreed to allow unexposed leaching tests as sufficient criteria for judging which samples can be exposed on scanners.<sup>2</sup>

### 3.4 Pre-Rinse to Partially Remove Leached Contaminants

The development of 193i resists is still in progress. The requirements of both low leaching and high resolution make resist development very difficult. For example, low activation energy resists are baked at low PEB temperatures and generally have smaller acid diffusion lengths, improving resolution, but tending to result in higher leaching levels.

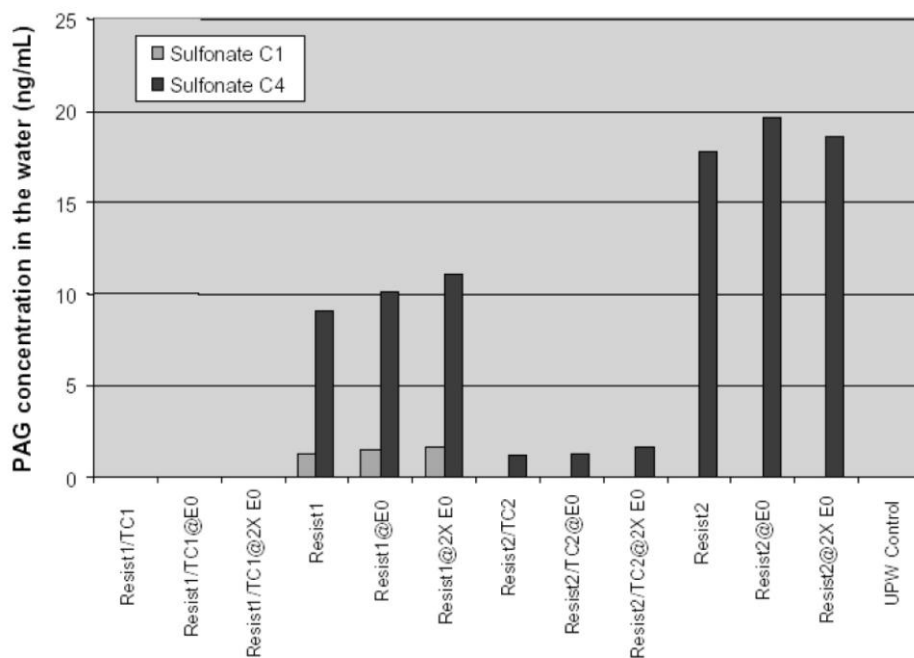


**Figure 3.7** Leaching tests of resist samples with and without topcoat under different exposure doses (detection limit  $\sim 0.2$  ng/mL). Sulfonate C1 is FC-122 and sulfonate C4 is PFBS.



Because some experimental resists exceed leaching thresholds, topcoats can be used to protect resists from leaching. Rinsing of the resist film by DI water before exposure has also been investigated as an alternative way to address this issue. DI-water rinses can wash away significant amounts of the leaching components. Leaching levels of pre-rinsed wafers can be reduced to ~12% of that of nonrinsed wafers. Similarly, the leaching time constant  $\beta$  can be decreased by a factor of about two.<sup>7</sup> Before the availability of low-leaching and high-performance 193i resists, “high leaching” 193-nm resists in combination with DI water pre-rinses were used. Figure 3.8 shows a typical process flow.

One major concern is the extent to which pre-rinse steps change resist sensitivity. To evaluate this, open frame exposures with a dose meander were carried out on wafers with different pre-rinse times of 0, 10, and 30 seconds. The maximum pre-rinse time of 30 seconds was selected, based on the assumption that leaching occurs within the first 30 seconds of water contact.<sup>13</sup> After development, the thickness of the remaining resist was measured as a function of dose. The resist thickness versus dose curves (contrast curves) shows no significant changes as a result of pre-rinse (Fig. 3.9). Similar results were obtained for a “dry” resist sample, which had a leaching level of ~24 ppb.

It is surprising that these contrast curves did not change with rinsing prior to exposure, since PAGs leach out of the film as soon as it contacts the water. We suspect that the flow of water through the exposure head provides the answer. The water is confined between the lens and the wafer. The water flow continues through the exposure head both during the exposure and between exposures. When the exposure head moves to the next die, before the exposure starts, the die is flushed by the water, providing an “intrinsic flush” prior to exposure.

According to simulation results,<sup>14</sup> this “intrinsic flush” occurs in about 1–2 seconds. Apparently, the intrinsic flush removes sufficient amounts of PAG from the resist prior to exposure so that the pre-rinse has no effect.

### 3.5 Lens Contamination Caused by Resist Leaching

Contamination of immersion water by the resist will in turn, contaminate the lens. During exposure to 193-nm light, components in the water may absorb photons and decompose into other chemical species. These chemical compounds may

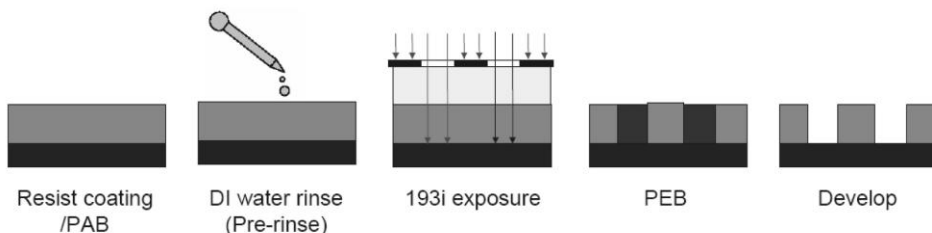
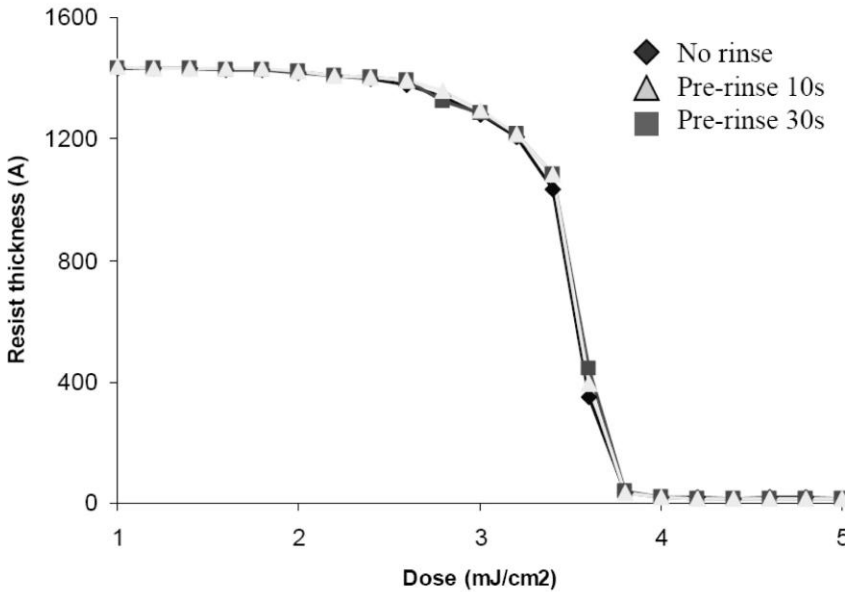


Figure 3.8 Process flow with pre-rinse.



**Figure 3.9** Contrast curves of a 193i resist with different pre-rinse times. The resist sample has a leaching of ~12 ppb.

have limited solubility in water and form deposits on the lens surface. Quantitative analysis of the leach-induced lens contamination is important to the design of immersion heads and for establishment of leaching specifications. Optimization of immersion head design should minimize contact between leaching components and lens, ultimately allowing for more relaxed leaching specifications for the resists.

### 3.5.1 Simulation results

In a simplified immersion system (Fig. 3.10(a)), water fills the gap between the lens and a wafer moving at a scan speed of ~500mm/s. A theoretic model from the University of Wisconsin was used to predict the concentration distribution of contaminants throughout the gap region.<sup>15</sup> The geometry of the gap is defined by its length ( $L = 4$  cm) and height ( $h = 1$  mm) (Fig. 3.10(a)).

Due to the concentration gradient and bulk fluid motion, the motion of contaminant species can be defined by the following flow equation (under the assumption of inertia-free and parallel flow):

$$\rho \frac{\partial u}{\partial t} = \mu \frac{\partial^2 u}{\partial y^2}, \quad (3.3)$$

where  $u$  is the velocity of water,  $\rho$  is the density of water, and  $\mu$  is the viscosity of water. The boundary conditions for Eq. (3.3) are  $u(y = 0, t) = \text{scan speed}$  (500

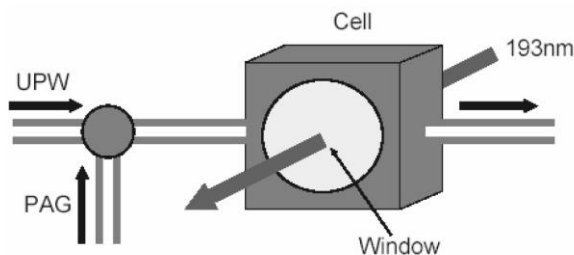
In reality, full-field immersion scanners have much more complicated immersion head designs than were described in the simplified model. In scanners, the injection and extraction of immersion water will most likely disturb the parallel flow described by the simplified model. Nonetheless, the qualitative conclusion that the chemicals leached from the resist will arrive at the lens within the timeframe of the exposure is relevant to the design of full-field scanners.

### 3.5.2 Controlled immersion contamination

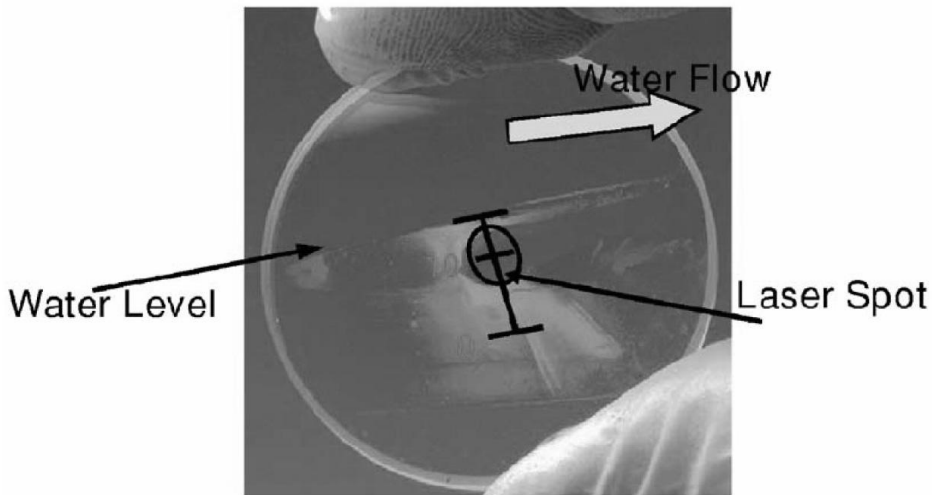
Irradiated by 193-nm photons, the chemical components in the water may decompose into water-insoluble species and deposit onto the lens surface, leading to transmission degradation of the lens. Controlled contamination experiments were designed to study lens contamination during exposure.<sup>16–19</sup> Figure 3.11 shows a diagram of the experimental setup. PAG as a contaminant was injected into ultrapure water (UPW) (18 M $\Omega$ -cm). This contaminated water flows through a cell with two windows. The windows are made from the 193-nm lens materials (fused silica or CaF<sub>2</sub>) with protective coatings. 193-nm light illuminates the water through the windows (Fig. 3.11). To accelerate the contamination process, the exposure dose is very high and the contaminant concentration is increased. After exposure, the transmission of the window is measured and the transmission loss is obtained.

Figure 3.12 shows the results reported by the MIT group.<sup>19</sup> In their experiment, the immersion cell has two 3-mm thick windows separated by a 2-mm gap. PAG (TPS-PFBS), which has a solubility of 2300 ppm in water, was tested. A syringe pump was used to inject PAG into the water upstream of the test cell, generating concentration levels of 3–3000 ppb. No deposition was observed without laser light, as the contamination precursor (PAG) is soluble in water. However, deposition of the contaminants did occur with exposure, but primarily *upstream* of the location of the 193-nm exposure area.

The authors offered the following explanation of the result.<sup>19</sup> The laser light initiates two opposing reactions: forward (contamination) and reverse (cleaning). During the forward reaction, the PAG undergoes photodecomposition, creating insoluble photoproducts. At the time of formation, these photoproducts diffuse to the surface of the windows, forming deposits. During the reverse reaction, the water photolyzes to form hydrogen peroxide (H<sub>2</sub>O<sub>2</sub>). H<sub>2</sub>O<sub>2</sub> can then react



**Figure 3.11** Setup of the controlled contamination experiment with 193-nm exposure.



**Figure 3.12** Contamination pattern formed after 193-nm exposure of 100 ppm of TPS-PFBS in water. (Reprinted by permission from Ref. 19.)

thermally or photochemically with the insoluble deposits to generate water-soluble products. In the directly exposed area, the dose is high, creating high concentrations of  $\text{H}_2\text{O}_2$ . The  $\text{H}_2\text{O}_2$  generated at the exposed area not only cleans the local contamination, but also flows downstream, cleaning the downstream areas. No difference was found between contamination of fused silica and coated  $\text{CaF}_2$  optics at the same exposure conditions.

Similar results were obtained by another group.<sup>18,20</sup> They also observed that the deposition of contaminants occurred primarily *around* the exposed areas, but not in the areas of highest exposure. Additionally, they found that contamination builds up at the immersion nozzle, resulting in increased pressure and decreased flow rate.

### 3.5.3 *In situ* cleaning of immersion systems

*In situ* cleaning is a process in which a cleaning solvent is injected into the immersion water so that it flows through the immersion system. The concept here the same as the concept in the controlled contamination experiment in Fig. 3.11. The cleaning solvent removes deposits and cleans the immersion water handling system. Depending on the purpose, various cleaning solvents can be used. For example, introducing  $\text{CO}_2$  gas into the immersion water flow can kill bacteria growing in the system. This type of cleaning is preferred from the customer's point of view, because the contaminated system can be cleaned without disassembling the exposure head and the water handling system, reducing downtime.

Figure 3.13 shows the results of one cleaning study using an apparatus similar to the one shown in Fig. 3.11.<sup>18,20</sup> The apparatus is filled with PAG-contaminated water and exposed across an area of  $2 \times 5 \text{ mm}^2$ . Transmittance is measured across an area of  $5 \times 10 \text{ mm}^2$ . The leaching components deposited on the lens are cleaned with a special lens-friendly cleaning fluid that is water soluble and has a neutral pH. Figure 3.13(b) shows the transmittance values measured before exposure, after exposure, and after *in situ* cleaning. Before exposure, the window has an average transmittance of  $\sim 83\%$ , however, after exposure the transmittance is reduced. The transmittance loss is related to the exposure dose and contaminant concentration. For the dose of 2.7 million pulses and a contaminant level of 10 ppm, a transmittance loss of 28% is observed. After exposure, the lens is flushed with the cleaning fluid for 10 minutes and most of the transmittance is recovered. For a dose of 4 million pulses and a contaminant level of 2 ppm, the transmittance loss from the light-contaminated lens is totally recovered after cleaning. Further spectral analysis indicates that the transmittance spectrum is completely recovered (Fig. 3.13(c)). In the case of more heavily contaminated lens, transmission loss cannot be completely recovered after the cleaning. These results show the importance of cleaning before too much contamination is deposited.

*In situ* cleaning can also remove deposits in water injection and extraction nozzles. Experiments have shown that water pressure, which increases with contamination, can be restored with *in situ* cleaning.<sup>20</sup>

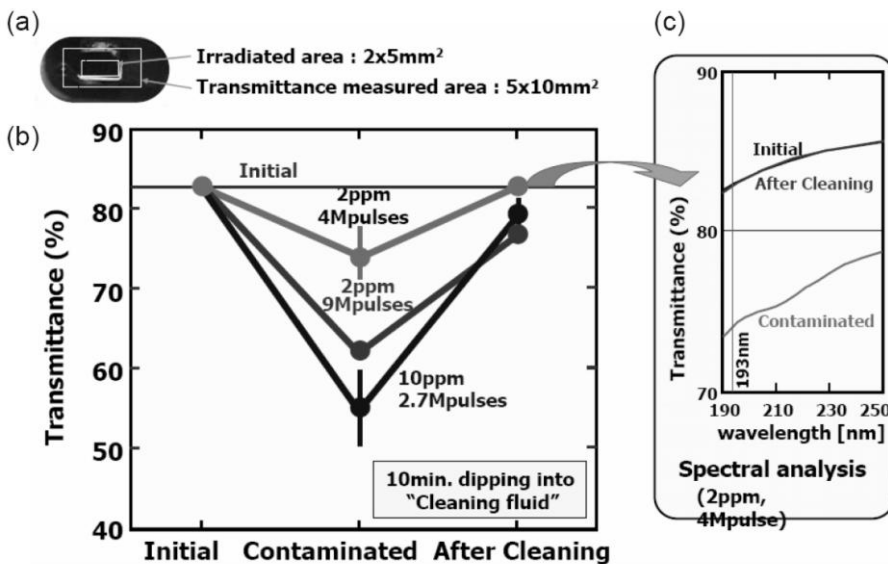


**Figure 3.13** Lens contamination and cleaning experiment. (a) Exposure area and transmittance measured area. (b) Transmittance values measured before exposure, after exposure, and after cleaning. Within the figure, the exposure dose and contaminant level are labeled. (c) Transmittance spectra of the window before exposure, after exposure with 2 million pulses and 2 ppm contaminant level, and after cleaning. (Reprinted by permission from Ref. 18.)

### 3.6 Water Uptake in Resist Film

In addition to the leaching of resist components into water, water can also diffuse into resist films, changing their reactivity. This water diffusion may occur even through a topcoat layer. Water may easily penetrate the topcoat layer and reach the resist film. This phenomenon can be explained by diffusion theory.

#### 3.6.1 Diffusion theory

Assuming that the diffusion of water in the resist film follows Fick's law, the diffusion behavior and water uptake can be modeled using the following equation:

$$\frac{M_t}{M_\infty} = 1 - \frac{8}{\pi^2} \sum_{n=0}^{\infty} \frac{i}{(2n+1)^2} \exp\left[-\frac{(2n+1)^2 \pi^2 D t}{L^2}\right], \quad (3.5)$$

where  $M_t$  is the mass uptake at time  $t$ ,  $M_\infty$  is the ultimate mass uptake at time  $t = \infty$ ,  $D$  is the water diffusion coefficient, and  $L$  is the film thickness.<sup>21,22</sup> At the initial phases of the diffusion process (for approximately  $M_t/M_\infty < 0.6$ ), Equation (3.5) can be simplified to a linear relationship versus the square root of time:

$$\frac{M_t}{M_\infty} = \frac{2}{L} \left( \frac{Dt}{\pi} \right)^{1/2}. \quad (3.6)$$

#### 3.6.2 Quartz crystal microbalance to measure water uptake

Water uptake by resist films can be experimentally measured using quartz crystal microbalances (QCMs). QCMs are piezoelectric transducers widely used in electrochemistry (Fig. 3.14(a)). Resonant frequency varies linearly with the mass of the device. The QCM converts from a change in mass ( $\Delta m$ ) to a change in resonant frequency ( $\Delta F$ ), which is an easily measured signal,

$$\Delta F = -k \Delta m, \quad (3.7)$$

where  $k$  is a coefficient and is dependent on the crystal and the circuit. This method is very useful because of its high mass sensitivity and can be used in real time to make *in situ* measurements. A frequency shift of 1 Hz corresponds to a mass change of 1 ng.